nature communications

Article

https://doi.org/10.1038/s41467-025-67788-0

Elevated atmospheric CO_2 decreases methylmercury production in freshwater lakes

Received: 12 November 2024

Accepted: 9 December 2025

Published online: 26 December 2025

Check for updates

Pei Lei[1,2,3,15], Jin Zhang[1,2,15], Ri-Qing Yu[4], Maciej Bartosiewicz[5,6], Chengjun Li[7], R. Iestyn Woolway[8], Martin Tsz-Ki Tsui[9], Tao Jiang[10], Bo Meng[11], Raymond W. M. Kwong[12], Yuming Guo[13], Huan He[1], Xinghui Xia[14], Hongqiang Ren[2] & Huan Zhong[2]

Elevated atmospheric carbon dioxide (CO_2) level reshapes microbial communities in nature, yet its consequences for neurotoxic methylmercury (MeHg) production in waters remain unclear. Here, we show that elevated CO_2 levels (650 and 1000 ppm) consistently reduced net MeHg production across 45 freshwater lakes spanning 1200 longitudinal kilometers, particularly in eutrophic conditions (54–96%). Elevated CO_2-driven shifts in carbon substrates favored hydrogenotrophic methanogens (e.g., *Methanobacterium*) lacking the *hgcA* methylation gene over *hgcA*-harboring acetoclastic strains (e.g., *Methanosarcina*), decreasing methanogen abundance (18–98% in *hgcA* copies) and activity (13–53% in net CH_4 production) and suppressing Hg methylation. Model simulations predict a 33%–74% global decline in lake MeHg production under future CO_2 scenarios, partially counteract MeHg increases associated with intensified algal blooms under warming. This overlooked pathway highlights the need to integrate interacting climate drivers to improve predictions of MeHg risks in a climate-changing future.

The biogeochemical cycling of the global pollutant mercury (Hg) is closely linked with methanogenesis[1–3], a primary process for organic matter decomposition that produces the potent greenhouse gas (GHG) of methane (CH_4)[4]. This connection is mainly due to methanogens, which are pivotal in methanogenesis and meanwhile act as essential microbes for Hg methylation[5], converting inorganic mercury (IHg) into neurotoxic methylmercury (MeHg). Consequently, changes in methanogens and methanogenesis significantly impact the MeHg production in natural waters and its subsequent accumulation in aquatic food chains, where MeHg can biomagnify up to ten million times[6] and lead to a demonstrable decrease in newborn intelligence quotient worldwide[7]. Particularly in eutrophic lakes, the

[1]School of Environment, Nanjing Normal University, Nanjing, China. [2]State Key Laboratory of Water Pollution Control and Green Resource Recycling, School of Environment, Nanjing University, Nanjing, China. [3]State Key Laboratory of Lake and Watershed Science for Water Security, Nanjing Institute of Geography and Limnology, Chinese Academy of Sciences, Nanjing, China. [4]Department of Biology, Center for Environment, Biodiversity and Conservation, The University of Texas at Tyler, Tyler, TX, USA. [5]Department of Environmental Sciences, University of Basel, Basel, Switzerland. [6]Institute of Geophysics, Polish Academy of Sciences, Warsaw, Poland. [7]Institute of Environmental Research at Greater Bay Area, Guangzhou University, Guangzhou, China. [8]School of Ocean Sciences, Bangor University, Bangor, UK. [9]School of Life Sciences, The Chinese University of Hong Kong, Hong Kong SAR, China. [10]Interdisciplinary Research Centre for Agriculture Green Development in Yangtze River Basin, College of Resources and Environment, Southwest University, Chongqing, China. [11]State Key Laboratory of Environmental Geochemistry, Institute of Geochemistry, Chinese Academy of Sciences, Guiyang, China. [12]Department of Biology, York University, Toronto, ON, Canada. [13]School of Public Health and Preventive Medicine, Monash University, Melbourne, VIC, Australia. [14]State Key Laboratory for Water Environment Simulation, School of Environment, Beijing Normal University, Beijing, China. [15]These authors contributed equally: Pei Lei, Jin Zhang. e-mail: zhonghuan@nju.edu.cn

decomposition of algal organic matter (AOM) increased the availability of labile carbon and CH_4 production by 16–44%, which was accompanied by a sharp spike in MeHg levels (1–2 orders of magnitude), primarily driven by methanogens[8]. Understanding the shifts in methanogen-mediated MeHg production in lakes is thus essential for predicting future risks of this potent neurotoxin in aquatic systems and its adverse impacts on wildlife and human health.

The composition and functions of methanogenic communities are impacted by the ambient levels of carbon dioxide (CO_2), a primary GHG with increasing atmospheric concentrations[9,10]. Crucially, this influence potentially extends to microbial MeHg production in water, which is a major source of MeHg in human food chains[11]. However, the cascading effects of elevated CO_2 on methanogenic communities in natural waters and hence on microbial MeHg production remain unclear. Evidence shows that elevated CO_2 levels increase the abundance of methanogens, with a 31–156% rise in rice paddies and 63–98% in marshes, leading to a 28–120% increase in CH_4 emissions[12,13]. Nevertheless, these changes may not directly apply to other natural waters, including freshwater lakes, due to differences in methanogen communities and their metabolic types across aquatic systems[4], with distinct capacities for Hg methylation[14]. For example, the acetoclastic methanogens, which use acetate as an energy substrate, predominate in agricultural wetlands[15], whereas hydrogenotrophic methanogens use H_2/CO_2, are more prevalent in freshwater lakes[16], yet their Hg methylation capacities differ[17]. Understanding how microbial MeHg production responds to elevated CO_2 is further complicated by the presence of a wide array of microbial groups, apart from methanogens, that co-contribute to MeHg formation, including sulfate-reducing bacteria (SRB) and iron-reducing bacteria (FeRB)[18]. In consequence of this complexity, existing knowledge of changes in methanogens under elevated CO_2 levels may not reliably predict concomitant changes in microbial MeHg production and its bioaccumulation in human food chains amid climate change.

Here, we aim to elucidate the effects of elevated CO_2 on Hg methylation in freshwaters, which are essential to aquaculture production, currently accounting for 77% of edible aquaculture production globally[19]. Particularly in Asia, human MeHg exposure was dominated by freshwater aquatic food intake, in addition to seafood[20]. Meanwhile, freshwater lakes are well-recognized hotspots for microbial MeHg production, a process significantly enhanced by eutrophication, which generates AOM upon algal decomposition[21] and thus provides carbon sources that boost the growth of Hg-methylating methanogens[8]. We thus quantified the net changes of MeHg in response to elevated atmospheric CO_2 levels (650 ppm and 1000 ppm) across 45 freshwater lakes spanning 1200 longitudinal kilometers along the Yangtze River in China. Results indicate that rising CO_2 levels consistently lead to a decline in both the abundance of Hg-methylating methanogens and net MeHg production. Global simulations, facilitated by our newly compiled dataset, reveal a crucial pathway through which the interplay of climatic factors helps reduce uncertainties in predicting MeHg risks in natural waters amid climate change. These discoveries deepen our understanding of global changes in distribution and risks of this potent neurotoxin under future scenarios.

Results and discussion

Reduced MeHg production in freshwater lakes under elevated CO_2

We demonstrate that elevated CO_2 concentrations inhibit MeHg production in freshwater lakes. This is achieved by quantifying net MeHg production in 45 freshwater lakes under various CO_2 and AOM levels (see Supplementary Table 1 for lake characteristics). As algal proliferation increases in response to nutrient enrichment, their biomass commonly serves as an indicator of nutrient abundance and eutrophication[22,23]. Therefore, microcosm experiments involving the addition of algal biomass to simulate eutrophic conditions provide a practical approach to studying MeHg production in eutrophic waters. Under ambient CO_2 levels, AOM markedly enhanced MeHg production, yielding 1–3 orders of magnitude higher levels across 45 lakes (Supplementary Fig. 1), likely driven by stimulated methanogenesis-mediated MeHg production[8,24]. Under the projected CO_2 level of 1000 ppm in the year 2100, corresponding to the high GHG emissions scenario (SSP5-8.5) outlined in the Sixth Assessment Report from Intergovernmental Panel on Climate Change[25], however, we observed a substantial and prevalent decrease in net MeHg production across the surveyed freshwater lakes. The reduction ranged from 14 to 96%, with an average decrease of 63% compared to ambient 420 ppm CO_2 conditions ($p < 0.05$, Fig. 1 and Supplementary Fig. 1). Similar trends were also evident for other projected CO_2 levels in 2100 (i.e., 650 ppm, corresponding to the SSP2-4.5 scenario with intermediate GHG emissions), where net MeHg production showed reductions ranging from 45 to 61% (Fig. 2a and Supplementary Fig. 2a).

Particularly, decline of MeHg production under elevated CO_2 levels was most pronounced under eutrophic conditions, simulated as high algal biomass additions. The most obvious decrease in net MeHg production (by 54–96%) was observed in microcosms incubated at 1000 ppm CO_2 and with added algal biomass (Fig. 1b). Furthermore, the CO_2-induced effect remained consistent across different amounts of AOM (i.e., "+200 Algae" to "+1000 Algae"), resulting in a reduction of MeHg from 26 to 93% ($p < 0.05$, Fig. 2b and Supplementary Fig. 2b). During the long-term (60-day) of algal decomposition in lake water with added algal biomass, the inhibition ranged from 60 to 93% with averaging 80% (Fig. 2c and Supplementary Fig. 2c).

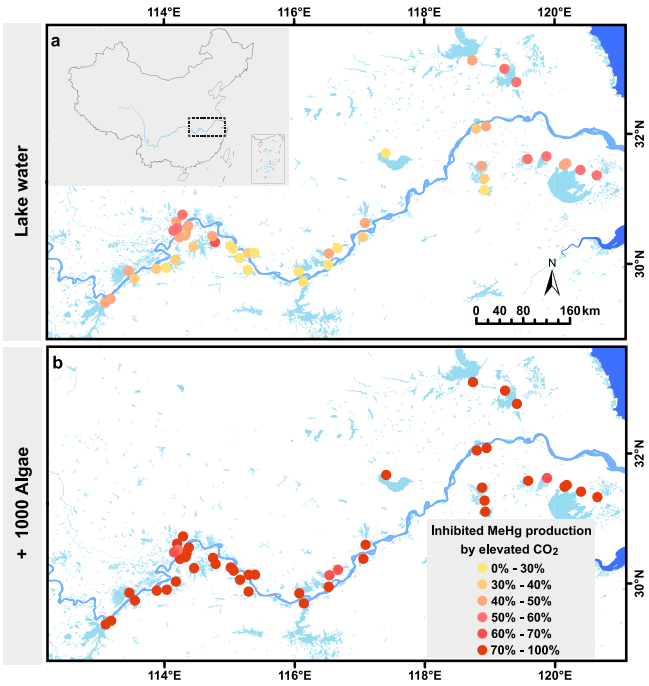

Fig. 1 | Elevated CO_2-inhibited MeHg production in lakes along the middle and lower reaches of the Yangtze River in China. a "Lake water": unfiltered lake water. **b** "+1000 Algae": unfiltered lake water amended with algal biomass to simulate bloom (resulting in approximately 1000 μg L^{-1} chlorophyll *a*) in Experiment A. Inhibited MeHg production by elevated CO_2 is denoted as the percentage changes of MeHg levels between "Ambient CO_2" and "Elevated CO_2." The map of the middle and lower reaches of the Yangtze River was generated using 1:1,000,000 National Fundamental Geographic Information Data of China (https://www.webmap.cn/commres.do?method=result100W). The inset map in the upper-left corner was produced on the basis of a licensed basemap (Map Approval Number: GS(2016)1569) provided by the Ministry of Natural Resources of China (http://bzdt.ch.mnr.gov.cn/).

https://doi.org/10.1038/s41467-025-67788-0

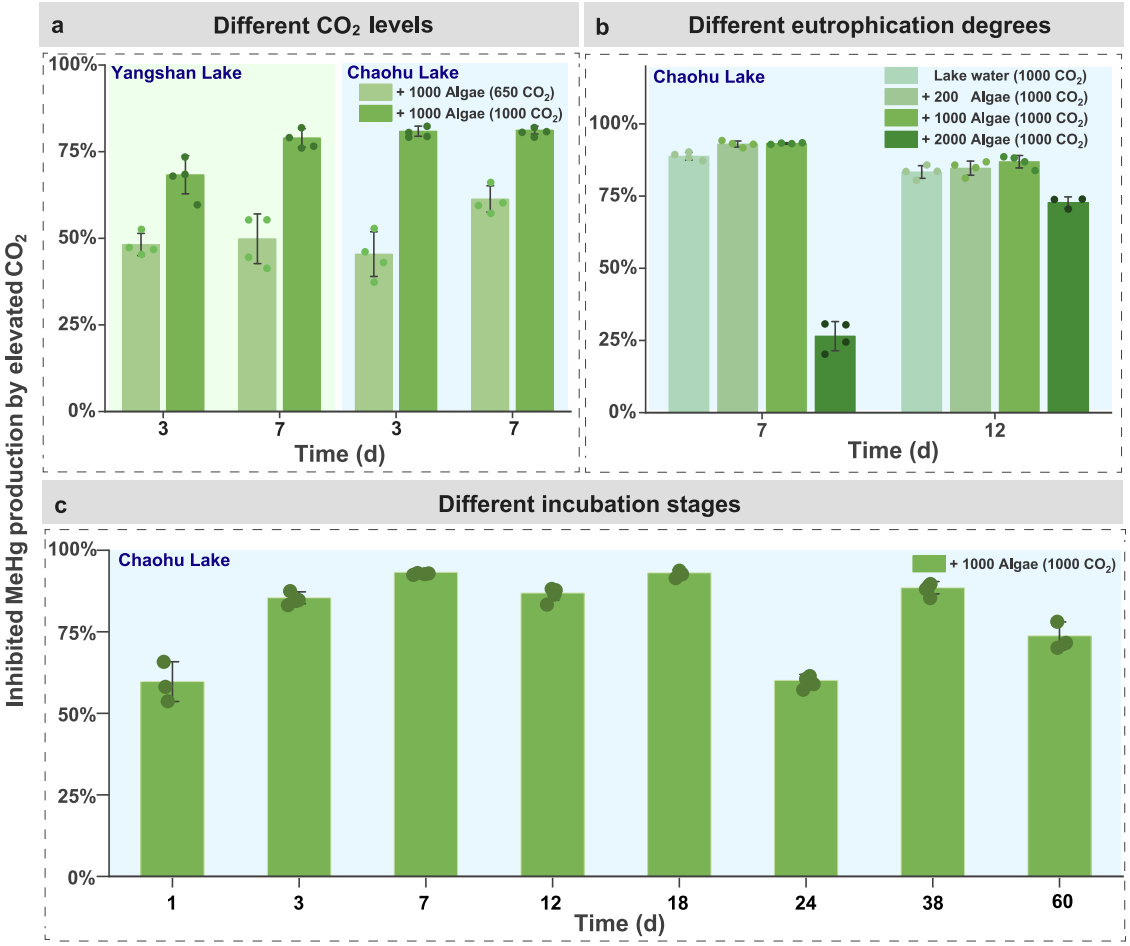

Fig. 2 | Elevated CO_2-inhibited MeHg production under different scenarios. **a** Inhibition rate of MeHg production under different elevated CO_2 levels (650 or 1000 ppm) compared to ambient 420 ppm CO_2. **b** Inhibition rate of MeHg production by elevated CO_2 (1000 ppm) compared to ambient CO_2 (420 ppm) under bloom intensities (200–2000 μg L^{-1} chlorophyll *a*). **c** Inhibition rate of MeHg production by elevated CO_2 (1000 ppm) compared to ambient CO_2 (420 ppm) under different stages of algal decomposition. "Lake water": unfiltered lake water. "+200 Algae," "+1000 Algae," and "+2000 Algae": unfiltered lake water (40 mL) amended with 0.001, 0.005, and 0.01 g of algal biomass, respectively. Before sampling on "Day 0," lake water was equilibrated for 4 h with Hg(II). Inhibited rate of MeHg production by elevated CO_2 are denoted as the percentage changes of MeHg levels between "Ambient CO_2" and "Elevated CO_2." Error bars show standard errors of the mean ($n = 3$ or 4). Each replicate is depicted as a circle on the bar, and details of each replicate can be found in the Source data.

We further extended the environmental relevance of elevated CO_2-impacted MeHg dynamics (see Supplementary Text 1). The CO_2-driven suppression of microbial Hg methylation is independent of background Hg levels, as shown by spiking experiments across a broad inorganic Hg (IHg) gradient (2–500 ng L^{-1}). Elevated CO_2 consistently reduced net MeHg production relative to ambient CO_2 levels, with 21–33% inhibition in unamended lake water and 66–83% in algal biomass-added treatments (Supplementary Fig. 3). We also established DOM gradients reflecting different autochthonous: allochthonous ratios (100:0 to 0:100; AOM vs. Soil organic matter, SOM). Results confirmed that AOM was a stronger driver of methylation than SOM, consistent with previous studies[8,26], and that elevated CO_2 significantly inhibited net MeHg production only when AOM comprised ≥50% of the DOM pool ($p < 0.001$; Supplementary Fig. 4), underscoring the need to clarify how DOM composition modulates CO_2-driven MeHg inhibition. Moreover, under combined climate forcing (elevated CO_2 and/or warming, $\Delta T = 4.4$ °C, SSP5-8.5 by 2100), MeHg production inhibition under "Elevated CO_2" and "Warming × Elevated CO_2" treatments (26–76% reduction) did not differ significantly ($p > 0.05$; Supplementary Fig. 5), indicating that the inhibitory effect of elevated CO_2 outweighs the stimulatory impact of warming, thus supporting the robustness of our model in projecting global MeHg trends. Importantly, such inhibition was also observed in other freshwater systems (e.g., 79% decrease in pond water; 75% in river water, Supplementary Fig. 6), suggesting that elevated CO_2 may mitigate MeHg risks across global inland waters. In summary, elevated CO_2 exerts a robust suppression of microbial MeHg production that is independent of background Hg levels, dependent on DOM sources, overrides warming effects, and extends broadly across freshwater systems.

Our results expand understanding of how elevated CO_2 reshapes Hg biogeochemistry and the associated risks of MeHg production, going beyond previous considerations of the impacts of CO_2 elevation on Hg toxicity[27], Hg bioaccumulation[28], and global Hg budgets[29]. To date, there has been relatively little focus on understanding the effect of elevated CO_2 on microbial MeHg production[30,31], the primary source of MeHg in human food chains. This knowledge gap is particularly critical in freshwater lakes, known as hotspots for MeHg formation[8,21] and sensitive to climate changes[32]. While recent studies indicate that AOM derived from algal decomposition in eutrophic lakes boosts microbial MeHg formation and inhibits its photodegradation[8,33], our study shows that such increases of MeHg levels in eutrophic waters would potentially be counteracted by future elevation in atmospheric CO_2 levels and thus inhibited Hg methylation. Implications of these processes are further discussed in the later sections.

https://doi.org/10.1038/s41467-025-67788-0

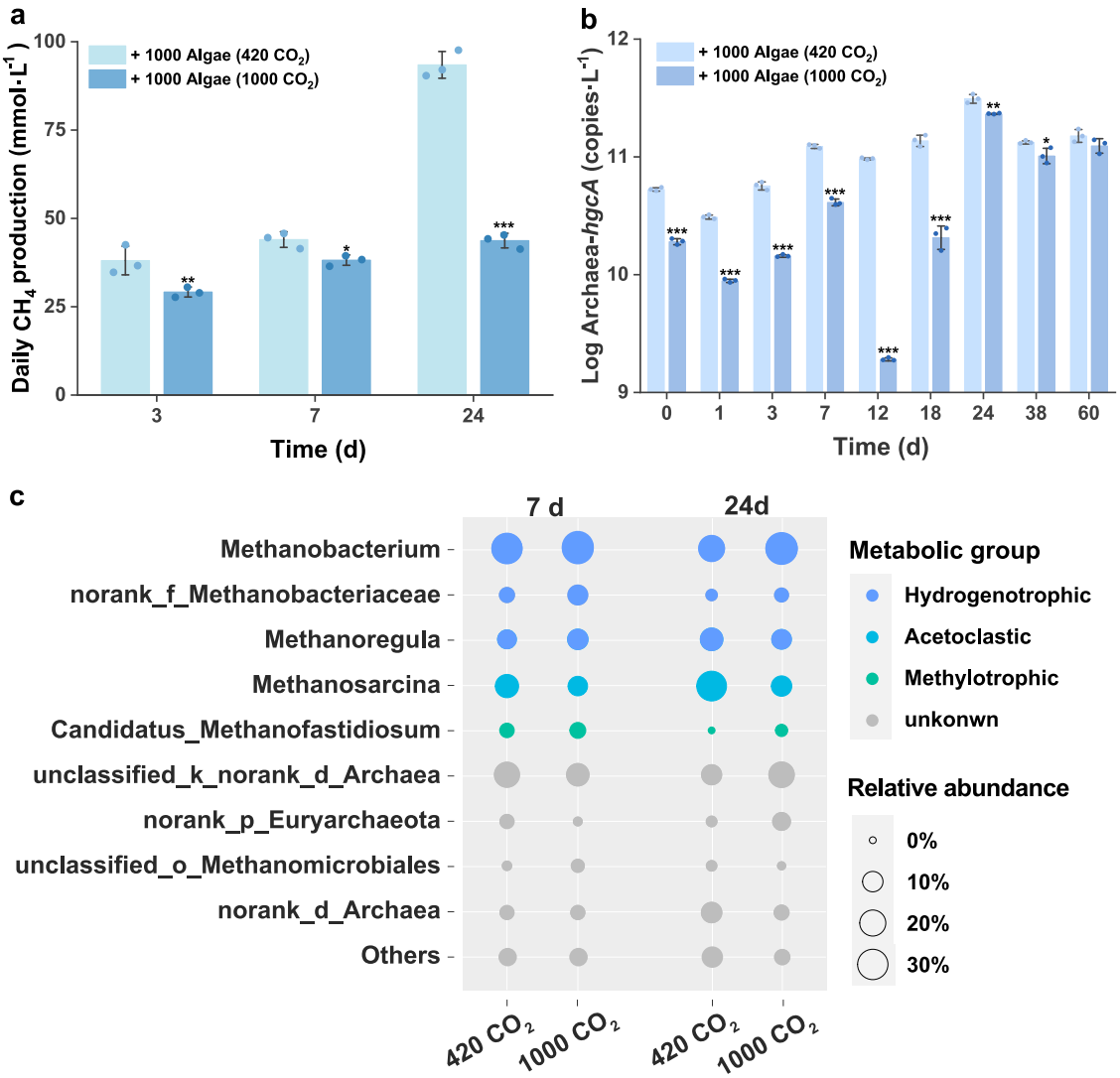

Fig. 3 | Activity, abundance, and metabolic types of methanogens are impacted by elevated CO_2. **a** Daily production of CH_4, **b** abundance of Archaea-*hgcA* genes, and **c** relative abundance of methanogens during the periods of algal decomposition under ambient CO_2 (420 ppm) or elevated CO_2 (1000 ppm) levels. Error bars show standard errors of the mean ($n = 3$).

The underlying mechanism by which elevated CO_2 levels inhibit Hg methylation in eutrophic waters

Given the more pronounced decreases in net MeHg production in eutrophic waters under elevated CO_2, we then focus on elucidating the mechanisms of such decreases under eutrophic conditions. Theoretically, the decrease in net MeHg production could be caused by decreased Hg methylation and/or increased MeHg demethylation[18]. Using Hg stable isotope tracing technique, we found that Hg methylation rates (k_m) were 83–89% lower under elevated CO_2 than under ambient conditions in both natural or eutrophic waters ($p < 0.001$), whereas MeHg demethylation rates (k_d) did not differ significantly between treatments (Supplementary Fig. 7). These complementary lines of evidence demonstrate that the observed decrease in net MeHg production lake water under elevated CO_2 was primarily attributed to inhibited Hg methylation, rather than the increases in MeHg demethylation. Consequently, we focused on how the dominant methylating microbes respond to elevated CO_2.

In eutrophic lakes, methanogens have been recognized as the key microbes for Hg methylation due to their higher relative abundances and increased activities facilitated by low-molecular weight AOM derived from algal decomposition[8]. Their enhanced activity significantly contributes to Hg methylation[34]. Therefore, changes in methanogens under elevated CO_2 offer a compelling explanation for the corresponding shifts in MeHg production in eutrophic waters. Our investigations demonstrate a substantial impact of elevated CO_2 on methanogenic activity, evidenced by the net daily CH_4 production rates. In eutrophic waters, these rates were considerably suppressed, averaging a 30% decrease with a range between 13 and 53% in comparison to the control under ambient CO_2 (Fig. 3a). Furthermore, the qPCR assays demonstrate that elevated CO_2 results in a decrease in copies of *hgcA*—as the Hg methylation gene—of Archaea by 18–98% (Fig. 3b), which are strongly correlated with the CO_2-inhibited MeHg production ($R^2_{adjust} = 0.866$, $p < 0.001$, Supplementary Fig. 8). These various pieces of evidence imply that methanogenetic activity and abundance are lowered under elevated CO_2, which provides an explanation for the inhibited microbial Hg methylation in eutrophic waters, where methanogens play a dominant role in MeHg production[8].

We further demonstrate that the observed MeHg decrease in eutrophic waters under elevated CO_2 could be explained by the shifting abundance of different metabolic types of methanogens, with an increase in weak or non-Hg methylating types and a decrease in strong Hg methylating counterparts. *Methanobacterium* spp., the most dominant group of methanogens in this study, is generally known as

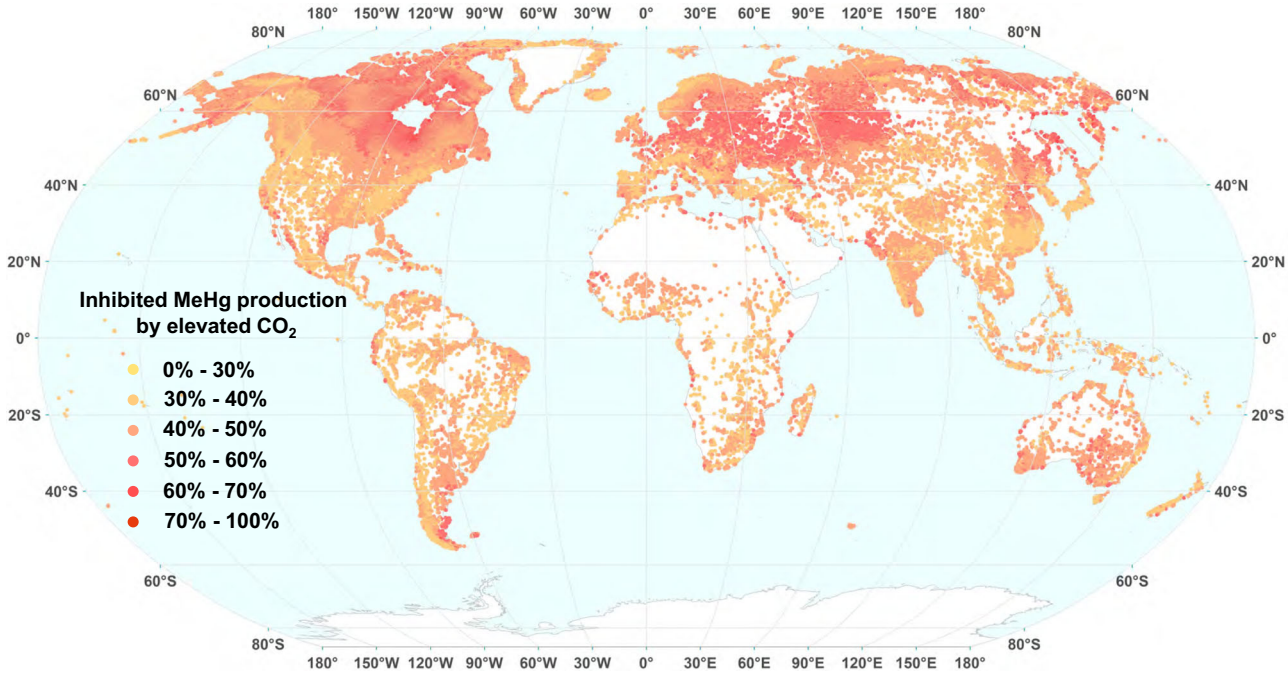

Fig. 4 | Projected decreases in MeHg production under elevated CO_2 conditions (1000 ppm in 2100) in global lakes. The predicted DOC concentrations in global lakes with a surface area larger than 0.1 km^2 were used (1,427,496 lakes in total, ranging from 0.0002 to 27.0 mg L^{-1}, with an average of 9.24 mg L^{-1}), and the database was obtained from a recent report[51]. The relationship between DOC and MeHg was adapted from a recent global meta-analysis[52]. The global map was obtained from Natural Earth dataset (https://www.naturalearthdata.com/downloads/10m-physical-vectors/).

hydrogenotrophic[35,36], while *Methanosarcina* is primarily known as acetoclastic methanogen[37]. High-throughput sequencing and bioinformatic analysis of *mcrA* genes revealed that elevated CO_2 leads to a notable shift in the methanogenic community: a decrease in the relative abundance of aceticlastic methanogens (e.g., *Methanosarcina* reduced from 29% in ambient CO_2 to 10% under elevated CO_2 on Day 24) and an increase in hydrogenotrophic methanogens (e.g., *Methanobacterium* increased from 22% in ambient CO_2 to 35% under elevated CO_2 on Day 24, Fig. 3c). Additional BLAST searches of *HgcAB* orthologs, indicates that among the 51 *HgcAB* orthologs identified in *Euryarchaeota*, 88% of potential Hg-methylating methanogens are associated with *Methanomicrobia*[38]. Within this taxon, primarily as the acetoclastic methanogen, *Methanosarcina* was observed in our samples. In contrast, hydrogenotrophic *Methanobacterium* spp., are much less likely to carry *hgcA* genes necessary for Hg methylation[38,39]. Consequently, we propose that the concomitant increase in hydrogenotrophic non-Hg methylating methanogens and the decrease in aceticlastic Hg methylating methanogens contributed to the reduced net MeHg production under elevated CO_2. This hypothesis requires further confirmation through a more quantitative comparisons of Hg methylation abilities across different methanogenetic taxa. Additionally, the interaction between methanogens and syntrophs, which has not been examined in this study, might play a role in modulating Hg methylation activities[40].

Such a transition from aceticlastic to hydrogenotrophic methanogens is ascribed to the changes in the predominant carbon sources under elevated CO_2 levels. In eutrophic lakes, the decomposition of planktonic biomass produces low-molecular-weight organic matter, e.g., aromatic proteins, stimulating aceticlastic methanogens[8]. These methanogens are possibly highly effective at utilizing bioavailable carbon and thrive across a broad range of environmental niches, including eutrophic lakes[41,42], which makes them key contributors in microbial MeHg production under eutrophic conditions[8]. However, elevated CO_2 levels, known as the preferred carbon source of hydrogenotrophic methanogens[43], might facilitate the growth of this metabolic type of methanogens, leading to a compositional shift from acetoclastic methanogens to hydrogenotrophic methanogens in eutrophic waters, a shift likely attributable to CO_2-stimulated fermentative H_2 production that relieves H_2 limitation and promotes hydrogenotrophic dominance (see detailed discussion in Supplementary Text 2). Similarly, elevated CO_2 increased the relative abundance of hydrogenotrophic methanogens (e.g., *Methanobacterium* and *Methanocella*) while significantly reducing the relative abundance of acetoclastic methanogens (e.g., *Methanosaeta*) in rice paddies[12]. An increase in the relative abundance of hydrogenotrophic methanogens was also reported in temperate marsh microcosms when exposed to elevated CO_2 levels[43].

In particular, the inhibited MeHg production under elevated CO_2 is unlikely due to other major Hg methylating microbes, such as SRB or FeRB, or possible changes in Hg bioavailability under elevated CO_2 due to acidification. Further discussion is presented in Supplementary Text 3.

Methanogens are widely distributed in natural environments where MeHg production occurs, including wetland soils, peatlands, freshwater, or marine sediments[44–46]. The key role of methanogens in Hg methylation, as well as their sensitivity to climatic factors, including elevated CO_2, global warming, and water acidification[10,47,48], highlight the urgency to elucidate and consider methanogen-mediated MeHg production in future climate change scenarios. Our results provide the initial evidence that the effects of climate change on methanogens would in turn affect microbial MeHg production, particularly in eutrophic waters subject to algal blooms, which are increasing under global warming[49,50]. Global implications of these findings are estimated and discussed in the following section.

Estimating how elevated CO_2 reduces MeHg levels in global lakes

To estimate the potential impact of the projected CO_2 elevation in 2100 (i.e., 1000 ppm[25]) on MeHg levels in global lakes, we coupled a relationship between elevated CO_2 and inhibited net MeHg production

in lakes with different ambient DOC contents, as established in this study (see Methods for details), and existing global datasets on (1) predicated[51,52] or (2) observational DOC and MeHg levels (summarized in Supplementary Data 1) in global lakes. Our simulations, based on global distribution of predicted DOC and MeHg, suggest that elevated CO_2 could lead to decreases in MeHg levels by 33–74% (average 47%) in lakes worldwide (Fig. 4). More specifically, in lakes characterized by high ambient DOC levels (averagely 18.7 mg L^{-1}) and high MeHg contents (averagely 0.61 ng L^{-1}), accounting for approximately 2.5% of the lakes examined, MeHg levels are projected to drop by 60–74% as CO_2 levels rise. Approximately one-third of the global lakes are anticipated to experience a reduction in MeHg levels between 30 and 45%, another third between 45 and 50%, whilst the remaining third will witness a decrease exceeding 50%. Similarly, inputting observed ambient DOC and MeHg concentrations—based on literature data (Supplementary Data 1)—into the same model predicts that elevated CO_2 could lead to a decrease in MeHg concentrations in lakes across the globe, ranging from 34 to 79%, with an average of 47%. Uncertainty analysis by Monte Carlo simulation shows that elevated CO_2 inhibits MeHg production in lakes worldwide, with an uncertainty range of 36–68% (Supplementary Text 4).

While the global reduction in MeHg levels under elevated CO_2 is estimated based on our modeling and found to be evident in lakes, it is important to note that there are numerous other factors that may influence the Hg methylation process in real-world scenarios, adding uncertainty to our estimates. More field studies quantifying the responses of MeHg production to changes in multiple climatic factors, including but not limited to CO_2 levels, are needed to further improve the reliability, and reduce the uncertainty of predicting MeHg levels in lakes in the context of climate change.

Environmental impacts: the interplay of climatic factors helps reduce uncertainties in MeHg risk prediction

Excessive nutrient inputs to lakes have led to a globally accelerated eutrophication, which in turn affects the magnitude, frequency, and duration of algal blooms[53]. Recent laboratory tests and field observations indicate that AOM in eutrophic lake waters promotes MeHg formation while reducing its photodegradation[8,33]. This contributes to MeHg accumulation in eutrophic lakes and increases the associated risks to wildlife and humans. Nevertheless, our findings demonstrate a counterbalancing effect from future climate change conditions: elevated atmospheric CO_2 mitigates methanogen-mediated Hg methylation in eutrophic waters, potentially offsetting the risks of global warming-amplified algal blooms[54] and hence enhanced Hg methylation[8].

Currently, predictions concerning Hg biogeochemistry and associated risks in the context of climate change commonly concentrate on the influence of individual climatic factors, such as rising CO_2[55] or global warming[56]. However, the interactive effects of multiple drivers are rarely assessed, partly because of the limited understanding of how the Hg cycle reacts to multiple simultaneous controlling processes. Our research highlights the potential for biased predictions concerning future Hg risks when considering a single climatic factor. This is because various climatic factors can exert conflicting influences on Hg biogeochemical cycles, as exemplified by the counteracting effects of CO_2 elevation and global warming—and hence algal blooms—on microbial MeHg production. Such a previously overlooked interplay of climatic factors can play a crucial role in stabilizing MeHg levels in natural settings amidst climate change. These combined effects should be incorporated into regional or global models of Hg biogeochemical cycles. Failing to acknowledge this unrecognized self-stabilization mechanism could lead to an overestimation of the impacts of climate change on MeHg risks (further detailed in Supplementary Text 5).

Interestingly, our experimental results indicate that the decrease in MeHg production under elevated CO_2 levels may extend from lakes to other freshwater systems, e.g., 79% decrease for pond water and 75% decrease for river water (see Supplementary Fig. 6). This implies that elevated CO_2 in the future could potentially mitigate MeHg formation on a broader scale, possibly affecting global inland freshwater systems that supply food to local populations and provide other critical ecosystem services[57]. Consequently, it is essential to address the crucial knowledge gaps related to the distinct and combined impacts of diverse climate facets on the production, accumulation, and transfer of MeHg in aquatic ecosystems. These insights serve as the foundation for developing more nuanced models of the Hg biogeochemical cycle, aiding in the prediction of the regional and global risk of MeHg to wildlife and humans.

More importantly, incorporating the combined effects of multiple climatic factors on the Hg cycle is key to reducing uncertainty in evaluating the effectiveness of our ongoing global Hg mitigation efforts. Currently, evaluating the effectiveness of Hg emission reductions under the Minamata Convention on Mercury is hindered by a significant disparity: while Hg emissions have been reduced, human exposure to MeHg has decreased at a much slower rate[7]. Per unit reduction in Hg emissions, human exposure has been estimated to decline by only one-third to one-half, reflecting the influence of complex processes such as legacy Hg in environmental reservoirs and bioaccumulation lags in food chains. This observed "mismatch"—where exposure decreases less than expected from emission reductions—likely arises from such multi-faceted drivers, including remobilization of legacy Hg by natural and anthropogenic factors[58].

Our study identifies a distinct climatic pathway that further complicates this emission–exposure relationship: elevated CO_2 suppresses microbial MeHg production in lakes, leading to reduced aquatic MeHg levels regardless of emission changes. This pathway would amplify the decline in human exposure beyond direct emission reductions, and should be accounted for when evaluating the effectiveness of global Hg mitigation efforts and interpreting temporal trends in biotic MeHg concentrations. Thus, our findings do not resolve the current mismatch, but rather reveal a previously unrecognized climate–microbe–MeHg interaction that may shape future exposure risks. Specifically, future increases in atmospheric CO_2 may counteract warming-driven enhancements of algal blooms, thereby reducing uncertainties in predicting aquatic MeHg risks under climate change. Incorporating this climate–microbe–Hg nexus into regional and global models of the biogeochemical cycling of Hg is crucial for reducing the uncertainty in the prediction of environmental MeHg concentrations under climate change scenarios. Such an improvement will substantially improve our ability to assess the effectiveness of the Minamata Convention on Mercury in mitigating MeHg exposure under the complex influence of multiple climatic factors.

Methods

Field sample collection

To examine the impacts of elevated CO_2 on MeHg production in lakes, we selected 45 freshwater lakes (No.1–45; 48 sampling sites, Supplementary Fig. 9 and Supplementary Table 1) spanning 1200 longitudinal kilometers in China. We also conducted laboratory microcosm experiments to characterize the kinetics of MeHg levels and the shifts in Hg methylating microbes under both ambient and elevated CO_2 conditions. These water samples were collected exclusively from the lakes along the middle and lower reaches of the Yangtze River, which constitute 28.6% of China's population and contribute 20.9% to the national Gross Domestic Product in 2018[59]. Many of these lakes experience anthropogenic eutrophication[60]. Lake water samples were gathered during the period from August to September in 2022.

At each sampling site, approximately 500 mL surface water samples were collected in triplicate at 0.5 m below the lake surface. Samples for Hg and nutrient analyses were preserved with 0.1% HCl, and the fresh unfiltered water was used for all microcosm experiments. All

water samples were stored in a dark, cold room (4 °C) until processing/analysis. Algal biomass samples were collected during the algal bloom period in August of 2022 from Chaohu Lake (31°42′48.94″N, 117°21′48.37″E), the fifth largest freshwater lake in China[8]. Briefly, at the lake, algal biomass was collected using a plankton net and stored at 4 °C until processing. Before experiments, algal biomass was washed, freeze-dried, and mortar-homogenized, and then stored at −20 °C prior to use. Samples for total mercury (THg), MeHg, and major nutrients were analyzed following established protocols (see Supplementary Fig. 10 for results).

Experimental microcosm setup

A series of microcosm experiments were designed to elucidate the effects and mechanisms of elevated CO_2 on microbial MeHg production in lake water. Specially, Experiments A to C aimed to reveal the general phenomenon of elevated CO_2 on microbial MeHg production under different conditions, such as different eutrophication scenarios or elevated CO_2 levels, by using diverse lake waters. Moreover, Experiment D was designed to elucidate the mechanisms of elevated CO_2-impacted MeHg production, and Experiment E was designed to explore whether elevated CO_2 affects the MeHg demethylation process. At the same time, MeHg levels were also determined for all processed incubation vials. The abundance of the *hgcA* genes in the mixture was quantified using the clade-specific degenerate primer pairs ORNL-Delta-HgcA and ORNL-Archaea-HgcA for *Deltaproteobacterial* methylators (e.g., SRB or FeRB) and Archaeal methylators (e.g., methanogens)[61], respectively (Supplementary Text 6). The quantification method for the relative abundances of acetoclastic to hydrogenotrophic methanogens was adopted from previous work (see Supplementary Text 7). Details of all treatments are summarized in Supplementary Table 2 and Text 8.

Determination of MeHg levels in water

The levels of dissolved MeHg were determined following the GEOTRACES protocol handbook[62]. The process involves adding 2 mL of the filtered sample to a 40 mL brown-glass bottle and adjusting the pH to 4 using a 2 M citrate buffer. A 2 mL sample volume was selected because, after the 7-day incubation, MeHg concentrations exceeded 0.2 ng L^{-1} in all treatments. Within the calibration curve range of 0.5–50 pg, this volume ensured accurate quantification. Subsequently, 50 µL of $NaBEt_4$ is added to the mixture. The solutions are then diluted with deionized water and measured using an automatic MeHg analyzer (CVAFS, Brooks Rand Model III, Brooks Rand Laboratories, USA) following Method 1630. Concentrations of MeHg were obtained using external calibration curves containing no less than 5 points ($r^2 > 0.999$). The detection limit for MeHg determinations was calculated as three times the standard deviation, the derived value being 0.01 ng L^{-1}. During the analyses of MeHg samples, quality assurance and quality control (QA/QC) measures were implemented, including the use of blanks, blank spikes, sample duplicates, and matrix spikes. Levels of MeHg were measured following daily calibration with a MeHg stock solution (MeHgCl source, 1 µg mL^{-1} in 0.5% HOAc, 0.2% HCl, 30 mL, Brooks Rand Laboratories, USA). Blank samples of ultrapure water and lake water from CHL without or with algal biomass addition were spiked with MeHg at an initial concentration of 10 ng L^{-1} ($n = 5$ for all treatments). The recovery percentages of MeHg standard analyses were 93% ± 7.3% and 96% ± 9.8% for the blank (ultrapure water) and lake water samples, respectively. For lake water added with AOM, the MeHg standards showed a recovery of 99% ± 10.9%. The recoveries of all spikes (ranging from 79 to 122%) fell within the acceptable range as outlined in the EPA Method 1630 (i.e., between 65 and 135% for MeHg, Supplementary Fig. 11).

Estimation of global MeHg reduction in lake water under elevated CO_2

To predict MeHg changes in response to elevated CO_2-induced MeHg production in water, we developed a global model for MeHg in lake water. This model relies on the observed drop in the MeHg production under elevated CO_2, as quantified in this study. Firstly, using data from Experiment A, we established that the relative reduction in MeHg production under elevated CO_2 in 45 lakes increases linearly with the rise of ambient DOC and MeHg contents (see Supplementary Table 3). Given that DOM in lake water has multiple sources (autochthonous and allochthonous), and that DOM from different sources exerts variable inhibitory effects on Hg methylation under elevated CO_2 (Supplementary Fig. 4), we incorporated this effect into our model predictions: for eutrophic waters, a mixture of autochthonous and allochthonous organic matter (AOM: SOM = 80%: 20%) was adopted in the model. Indeed, the decline in MeHg production rate (%) under elevated CO_2 can be calculated as: R (Inhibited rate of MeHg (%) by elevated CO_2) = (0.015 ± 0.003) × [DOC] + (0.01 ± 0.001) × [MeHg] + (0.333 ± 0.027), $r^2_{adjust} = 0.701$, $p < 0.001$, [DOC] < 30 mg L^{-1}, where ±SE is the standard error of the fit and is considered one of the uncertainties in the model and r^2_{adjust} is the correlation coefficient of the relationship. The above relationships are statistically significant ($p < 0.001$). The DOC in "Lake water + Algae" treatments can be estimated as: $[DOC]_{Lake\ water+algal\ biomass} = (1.389 \pm 0.075) \times [DOC]_{lake\ water} + (6.4 \pm 0.638)$ ($r^2_{adjust} = 0.991$, $p = 0.003$, see Supplementary Fig. 12a).

Subsequently, we estimated global MeHg reduction under elevated CO_2 using two independent databases: (1) global data on the predicated DOC[51] and MeHg levels[52] or observational ambient DOC and MeHg levels in global lakes. For the first one, predicted DOC concentrations in global lakes with a surface area larger than 0.1 km^2 were used (1,427,496 lakes in total, ranging from 0.0002 to 27.0 mg L^{-1}, with an average of 9.24 mg L^{-1})[51]. Using the relationship between DOC and MeHg from Lavoie et al.[52], we calculated the MeHg concentrations of 1,427,496 lakes globally: $[MeHg]_{Asia} = 0.004 \times [DOC] - 0.022$; $[MeHg]_{Europe} = 0.015 \times [DOC] + 0.156$; $[MeHg]_{North\ America} = 0.045 \times [DOC] - 0.158$. The global average slope and intercept were used to represent the relationship between MeHg and DOC concentrations in lakes located in other continents (including South America, Oceania, and Africa), i.e., $[MeHg]_{others} = 0.029 \times [DOC] - 0.019$. The average concentration of calculated MeHg was 0.27 ng L^{-1}. This dataset covers sites spanning six continents and a broad latitudinal range. Eventually, MeHg concentrations in global lake water bodies were predicted at the anticipated CO_2 concentration of 1000 ppm in 2100, utilizing the formula and data.

For the second database, we systematically reviewed literature spanning the period from 2000 to 2023 that documented MeHg and DOC levels in lakes (Web of Science™ search on June 6, 2023). From the search results of 201 scientific papers, we obtained 49 articles containing 229 samples for analyses (see Supplementary Data 1). These data were selected according to specific criteria: (i) inclusion of only field sampling data; (ii) acquisition of both unfiltered and filtered water samples; (iii) utilization of data from the most recent year collected at the same sampling point, and (iv) restriction of DOC concentrations to no more than 30 mg L^{-1}. More specifically, this dataset comprises 74 water samples that exclusively display unfiltered total MeHg values, 88 water samples exclusively exhibiting filtered MeHg values, and 67 water samples providing both unfiltered and filtered MeHg values. Notably, linear regression analyses revealed a significant relationship between filtered and unfiltered total MeHg levels present in water: $[MeHg]_{filtered} = (0.708 \pm 0.015) \times [MeHg]_{unfiltered} - (0.001 \pm 0.004)$, $r^2_{adjust} = 0.972$, $p < 0.001$ (see Supplementary Fig. 12b). The fitting errors mentioned above were considered as the uncertainty of the model. Accordingly, filtered MeHg concentrations in the 74 water samples lacking such data were calculated using the formula above. The average concentrations of DOC and MeHg in 229 lake water samples were 9.51 mg L^{-1} and 0.14 ng L^{-1}, respectively. This dataset covering lakes spanning five continents was used to predict MeHg concentrations under the future CO_2 concentration (1000 ppm).

Data availability

Source data are provided with this paper.

References

1. Blum, P. W., Hershey, A. E., Tsui, M. T. K., Hammerschmidt, C. R. & Agather, A. M. Methylmercury and methane production potentials in North Carolina Piedmont stream sediments. *Biogeochemistry* **137**, 181–195 (2018).
2. Wu, Q. et al. Methanogenesis is an important process in controlling MeHg concentration in rice paddy soils affected by mining activities. *Environ. Sci. Technol.* **54**, 13517–13526 (2020).
3. Liu, Y. W. et al. Atmospheric Hg(0) dry deposition over environmental surfaces: Insights from mercury isotope fractionation. *Eco-Environ. Health* **3**, 543–555 (2024).
4. Conrad, R. Importance of hydrogenotrophic, aceticlastic and methylotrophic methanogenesis for methane production in terrestrial, aquatic and other anoxic environments: a mini review. *Pedosphere* **30**, 25–39 (2020).
5. Hamelin, S., Amyot, M., Barkay, T., Wang, Y. & Planas, D. Methanogens: principal methylators of mercury in lake periphyton. *Environ. Sci. Technol.* **45**, 7693–7700 (2011).
6. Motta, L. C. et al. Mercury isotopic evidence for the importance of particles as a source of mercury to marine organisms. *Proc. Natl. Acad. Sci. USA* **119**, e2208183119 (2022).
7. Zhang, Y. X. et al. Global health effects of future atmospheric mercury emissions. *Nat. Commun.* **12**, 3035 (2021).
8. Lei, P. et al. Algal organic matter drives methanogen-mediated methylmercury production in water from eutrophic shallow lakes. *Environ. Sci. Technol.* **55**, 10811–10820 (2021).
9. Lin, Y. X. et al. Divergent responses of wetland methane emissions to elevated atmospheric CO_2 dependent on water table. *Water Res.* **205**, 117682 (2021).
10. Wang, Y. Y. et al. The process of methanogenesis in paddy fields under different elevated CO_2 concentrations. *Sci. Total Environ.* **773**, 145629 (2021).
11. Liu, M. D. et al. Rivers as the largest source of mercury to coastal oceans worldwide. *Nat. Geosci.* **14**, 672–677 (2021).
12. Wang, C. et al. An additive effect of elevated atmospheric CO_2 and rising temperature on methane emissions related to methanogenic community in rice paddies. *Agric. Ecosyst. Environ.* **257**, 165–174 (2018).
13. Lin, Y. X., Liu, D. Y., Yuan, J. J., Ye, G. P. & Ding, W. X. Methanogenic community was stable in two contrasting freshwater marshes exposed to elevated atmospheric CO_2. *Front. Microbiol.* **8**, 932 (2017).
14. Gilmour, C. C., Bullock, A. L., McBurney, A., Podar, M. & Elias, D. A. Robust mercury methylation across diverse methanogenic Archaea. *Mbio* **9**, 10–1128 (2018).
15. Alpana, S., Vishwakarma, P., Adhya, T. K., Inubushi, K. & Dubey, S. K. Molecular ecological perspective of methanogenic archaeal community in rice agroecosystem. *Sci. Total Environ.* **596**, 136–146 (2017).
16. Yang, Y. Y., Chen, J. F., Tong, T. L., Xie, S. G. & Liu, Y. Influences of eutrophication on methanogenesis pathways and methanogenic microbial community structures in freshwater lakes. *Environ. Pollut.* **260**, 114106 (2020).
17. Hao, Z. et al. Relative importance of aceticlastic methanogens and hydrogenotrophic methanogens on mercury methylation and methylmercury demethylation in paddy soils. *Sci. Total Environ.* **906**, 167601 (2023).
18. Lei, P. et al. Properly interpret metabolic inhibition results to identify primary mercury methylating microbes. *Crit. Rev. Environ. Sci. Technol.* **53**, 1757–1773 (2023).
19. Zhang, W. et al. Aquaculture will continue to depend more on land than sea. *Nature* **603**, E2–E4 (2022).
20. Liu, M. et al. Impacts of farmed fish consumption and food trade on methylmercury exposure in China. *Environ. Int.* **120**, 333–344 (2018).
21. Wang, T. T. et al. MeHg production in eutrophic lakes: focusing on the roles of algal organic matter and iron-sulfur-phosphorus dynamics. *J. Hazard. Mater.* **457**, 131682 (2023).
22. Tang, Y., Zhang, M., Sun, G. & Pan, G. Impact of eutrophication on arsenic cycling in freshwaters. *Water Res.* **150**, 191–199 (2019).
23. Bai, L. L. et al. Toward quantitative understanding of the bioavailability of dissolved organic matter in freshwater lake during *Cyanobacteria* blooming. *Environ. Sci. Technol.* **51**, 6018–6026 (2017).
24. Herrero Ortega, S. et al. High methylmercury formation in ponds fueled by fresh humic and algal derived organic matter. *Limnol. Oceanogr.* **63**, 544–553 (2018).
25. IPCC. *Climate Change 2023: Sixth Assessment Report (AR6)* https://www.ipcc.ch/report/ar6/syr/ (Intergovernmental Panel on Climate Change, 2023).
26. Wu, Z. Y. et al. Differential response of Hg-methylating and MeHg-demethylating microbiomes to dissolved organic matter components in eutrophic lake water. *J. Hazard. Mater.* **465**, 133298 (2024).
27. Wei, H., Xie, D. M., Wang, D. Z. & Wang, M. H. A meta-analysis reveals global change stressors potentially aggravate mercury toxicity in marine biota. *Environ. Sci. Technol.* **58**, 219–230 (2023).
28. Gentès, S. et al. In vivo mercury (de)methylation metabolism in cephalopods under different pCO_2 scenarios. *Environ. Sci. Technol.* **57**, 5761–5770 (2023).
29. Yuan, T. et al. Potential decoupling of CO_2 and Hg uptake process by global vegetation in the 21st century. *Nat. Commun.* **15**, 4490 (2024).
30. Strickman, R. J. et al. Effects of elevated CO_2 on MeHg and IHg in rice. *Environ. Adv.* **16**, 100515 (2024).
31. Wu, D. N. et al. Elevated CO_2 exacerbates the risk of methylmercury exposure in consuming aquatic products: evidence from a complex paddy wetland ecosystem. *Environ. Pollut.* **352**, 124095 (2024).
32. Woolway, R. I. et al. Global lake responses to climate change. *Nat. Rev. Earth Environ.* **1**, 388–403 (2020).
33. Lei, P. et al. Algal organic matter inhibits methylmercury photodegradation in eutrophic lake water: a dynamic study. *Sci. Total Environ.* **899**, 165661 (2023).
34. Christensen, G. A. et al. Carbon amendments alter microbial community structure and net mercury methylation potential in sediments. *Appl. Environ. Microbiol.* **84**, e01049–01017 (2018).
35. Kern, T., Linge, M. & Rother, M. *Methanobacterium aggregans* sp nov., a hydrogenotrophic methanogenic archaeon isolated from an anaerobic digester. *Int. J. Syst. Evol. Microbiol.* **65**, 1975–1980 (2015).
36. Kitamura, K., Fujita, T., Akada, S. & Tonouchi, A. *Methanobacterium kanagiense* sp nov., a hydrogenotrophic methanogen, isolated from rice-field soil. *Int. J. Syst. Evol. Microbiol.* **61**, 1246–1252 (2011).
37. Beckmann, S. & Manefield, M. Acetoclastic methane formation from *Eucalyptus* detritus in pristine hydrocarbon-rich river sediments by *Methanosarcinales*. *FEMS Microbiol. Ecol.* **90**, 587–598 (2014).
38. Yu, R.-Q. & Barkay, T. Microbial mercury transformations: molecules, functions and organisms. *Adv. Appl. Microbiol.* **118**, 31–90 (2022).
39. Yu, R.-Q., Reinfelder, J. R., Hines, M. E. & Barkay, T. Mercury methylation by the methanogen *methanospirillum hungatei*. *Appl. Environ. Microbiol.* **79**, 6325–6330 (2013).
40. Yu, R. Q., Reinfelder, J. R., Hines, M. E. & Barkay, T. Syntrophic pathways for microbial mercury methylation. *ISME J* **12**, 1826–1835 (2018).
41. Schwarz, J. I. K., Eckert, W. & Conrad, R. Response of the methanogenic microbial community of a profundal lake sediment (Lake Kinneret, Israel) to algal deposition. *Limnol. Oceanogr.* **53**, 113–121 (2008).

42. Schulz, S. & Conrad, R. Effect of algal deposition on acetate and methane concentrations in the profundal sediment of a deep lake (Lake Constance). *FEMS Microbiol. Ecol.* **16**, 251–259 (1995).
43. Lee, S. H., Kim, S. Y. & Kang, H. Effects of elevated CO_2 on communities of denitrifying bacteria and methanogens in a temperate marsh microcosm. *Microb. Ecol.* **64**, 485–498 (2012).
44. Weber, T., Wiseman, N. A. & Kock, A. Global ocean methane emissions dominated by shallow coastal waters. *Nat. Commun.* **10**, 4584 (2019).
45. Yakimovich, K. M. et al. Lake characteristics influence how methanogens in littoral sediments respond to terrestrial litter inputs. *ISME J.* **14**, 2153–2163 (2020).
46. Zhang, C. J., Pan, J., Liu, Y., Duan, C. H. & Li, M. Genomic and transcriptomic insights into methanogenesis potential of novel methanogens from mangrove sediments. *Microbiome* **8**, 94 (2020).
47. Yvon-Durocher, G. et al. Methane fluxes show consistent temperature dependence across microbial to ecosystem scales. *Nature* **507**, 488–491 (2014).
48. Yasin, N. H. M. et al. Oceans as bioenergy pools for methane production using activated methanogens in waste sewage sludge. *Appl. Energy* **202**, 399–407 (2017).
49. Visser, P. M. et al. How rising CO_2 and global warming may stimulate harmful cyanobacterial blooms. *Harmful Algae* **54**, 145–159 (2016).
50. Wang, J. M. et al. Comprehensive evaluation framework for intervention on health effects of ambient temperature. *Eco-Environ. Health* **3**, 154–164 (2024).
51. Toming, K. et al. Predicting lake dissolved organic carbon at a global scale. *Sci. Rep.* **10**, 8471 (2020).
52. Lavoie, R. A., Amyot, M. & Lapierre, J. F. Global meta-analysis on the relationship between mercury and dissolved organic carbon in freshwater environments. *J. Geophys. Res. Biogeosci.* **124**, 1508–1523 (2019).
53. Huisman, J. et al. Cyanobacterial blooms. *Nat. Rev. Microbiol.* **16**, 471–484 (2018).
54. Ho, J. C., Michalak, A. M. & Pahlevan, N. Widespread global increase in intense lake phytoplankton blooms since the 1980s. *Nature* **574**, 667–670 (2019).
55. Tang, B., Chen, J., Wang, Z. W., Qin, P. F. & Zhang, X. S. Mercury accumulation response of rice plant (*Oryza sativa L.*) to elevated atmospheric mercury and carbon dioxide. *Ecotoxicol. Environ. Saf.* **224**, 112628 (2021).
56. Zhao, W. W., Xin, Y., Zhang, Z. S., Zhang, X. H. & Wu, H. T. Accelerated Hg loss and increased methylmercury covary with soil organic matter mineralization and dissolved organic matter humification under warming conditions in permafrost marsh, Northeast China. *Environ. Res.* **234**, 116593 (2023).
57. Rodell, M. et al. Emerging trends in global freshwater availability. *Nature* **557**, 651–659 (2018).
58. Sun, R. Y. et al. Mercury isotope variations in lake sediment cores in response to direct mercury emissions from non-ferrous metal smelters and legacy mercury remobilization. *Environ. Sci. Technol.* **56**, 8266–8277 (2022).
59. Yu, X. B., Li, C. L., Huo, T. Z. & Ji, Z. H. Information diffusion theory-based approach for the risk assessment of meteorological disasters in the Yangtze River Basin. *Nat. Hazards* **107**, 2337–2362 (2021).
60. Huang, J. et al. How successful are the restoration efforts of China's lakes and reservoirs?. *Environ. Int.* **123**, 96–103 (2019).
61. Liu, Y., Delgado-Baquerizo, M., Bi, L., Zhu, J. & He, J. Consistent responses of soil microbial taxonomic and functional attributes to mercury pollution across China. *Microbiome* **6**, 183 (2018).
62. Cuttler, G. et al. Sampling and sample-handling protocols for GEOTRACES cruises. GEOTRACES. https://geotracesold.sedoo.fr/images/Cookbook.pdf (2017).

Acknowledgements

This work was supported by the National Natural Science Foundation of China (NSFC; Grant Nos. 42525710 to H.Z., 42477399 and 42107383 to P.L.) and by the State Key Laboratory of Lake Province and Watershed Science for Water Security (Grant No. 2024SKL012 to P.L.). The authors gratefully acknowledge Shizhong Lei, Zhuoran Li, Dr. Sheng Guo, and Dr. Chao Wang for their valuable assistance with field water sample collection.

Author contributions

P.L. and H.Z. conceptualized the study and provided overall supervision. J.Z. developed the methodology and prepared the figures. P.L., R.Y., M.B., and R.W. contributed to data validation. P.L. and J.Z. conducted the investigation. P.L., J.Z., and C.L. performed data curation. P.L. and J.Z. drafted the original manuscript. P.L. and H.Z. acquired the funding. M.T., T.J., B.M., R.K., Y.G., H.H., X.X., H.R., and H.Z. contributed to result interpretation and reviewed the manuscript.

Competing interests

The authors declare no competing interests.

Additional information

Supplementary information The online version contains supplementary material available at https://doi.org/10.1038/s41467-025-67788-0.

Correspondence and requests for materials should be addressed to Huan Zhong.

Peer review information *Nature Communications* thanks Kevin Bishop and the other, anonymous, reviewer(s) for their contribution to the peer review of this work. A peer review file is available.

Reprints and permissions information is available at http://www.nature.com/reprints

Publisher's note Springer Nature remains neutral with regard to jurisdictional claims in published maps and institutional affiliations.

Open Access This article is licensed under a Creative Commons Attribution 4.0 International License, which permits use, sharing, adaptation, distribution and reproduction in any medium or format, as long as you give appropriate credit to the original author(s) and the source, provide a link to the Creative Commons licence, and indicate if changes were made. The images or other third party material in this article are included in the article's Creative Commons licence, unless indicated otherwise in a credit line to the material. If material is not included in the article's Creative Commons licence and your intended use is not permitted by statutory regulation or exceeds the permitted use, you will need to obtain permission directly from the copyright holder. To view a copy of this licence, visit http://creativecommons.org/licenses/by/4.0/.

© The Author(s) 2025